Journix: Journal of Informatics and Computing
Vol. 1 No. 3, 2025 : 120-134
ISSN : 3090-6784 | DOI : 10.63866/journix.v1i3.9

FCM-Guided CNN with Fuzzy Membership Maps for Robust Brain MRI Tumor Classification

Firnanda Al-Islama Achyunda Putra [1*], Kukuh Yudhistiro [1], Sutriawan [2], Zumhur Alamin [2]

[1] Universitas Merdeka Malang
[2] Universitas Muhammadiyah Bima

Email: firnanda.putra@unmer.ac.id
(* : corresponding author)

ABSTRACT – Accurate brain MRI classification is critical for early tumor diagnosis and computer-aided clinical decision support. Conventional convolutional neural networks (CNNs) are effective in learning deep hierarchical features but often struggle with intensity heterogeneity and partial volume effects inherent to MRI data. To address these limitations, this study proposes a hybrid Fuzzy C-Means–CNN (FCM–CNN) framework that integrates unsupervised soft clustering with deep feature learning. The fuzzy segmentation stage preserves boundary uncertainty by generating multi-channel membership maps, which are then fed into a CNN for robust classification. Evaluations conducted on the Kaggle brain MRI dataset (3,264 slices across four diagnostic categories) under Stratified 5-Fold Cross-Validation show consistent improvements over baseline models. The proposed FCM–CNN achieves a mean accuracy of 96.26% and Macro-F1 of 0.9622, surpassing both CNN-only and K-Means+CNN by +4.84% and +2.74% respectively. Ablation analysis confirms that soft memberships enhance discrimination between visually similar tumors, while statistical testing verifies that the gains are systematic and reproducible. Furthermore, the fuzzy membership maps provide interpretable visual cues, aligning with recent trends in explainable AI (XAI) for medical imaging. Overall, the FCM–CNN framework demonstrates that combining fuzzy logic with deep learning yields a balanced trade-off between performance, interpretability, and computational efficiency, making it promising for clinical-grade brain MRI analysis.

KEYWORDS: Fuzzy C-Means, Convolutional Neural Network, Brain MRI Classification, Medical Image Analysis, Explainable AI

CNN Terpandu FCM dengan Peta Keanggotaan Fuzzy untuk Klasifikasi Tumor MRI Otak yang Robust

ABSTRAK – Klasifikasi citra MRI otak yang akurat berperan penting dalam diagnosis dini tumor dan pengambilan keputusan klinis berbantuan komputer. Meskipun Convolutional Neural Network (CNN) mampu mengekstraksi fitur hierarkis yang mendalam, model ini sering mengalami penurunan kinerja akibat heterogenitas intensitas dan efek volume parsial pada citra MRI. Untuk mengatasi hal tersebut, penelitian ini mengusulkan kerangka hibrida Fuzzy C-Means–CNN (FCM–CNN) yang menggabungkan klasterisasi lembut tanpa pengawasan dengan pembelajaran fitur mendalam. Tahap segmentasi fuzzy mempertahankan ketidakpastian batas jaringan dengan menghasilkan peta keanggotaan multikanal, yang kemudian digunakan sebagai masukan bagi CNN untuk klasifikasi yang lebih tangguh. Evaluasi menggunakan dataset MRI otak dari Kaggle (3.264 irisan, empat kategori

diagnostik) dengan Stratified 5-Fold Cross-Validation menunjukkan peningkatan kinerja yang konsisten dibandingkan model dasar. Metode FCM–CNN mencapai akurasi rata-rata 96,26% dan Macro-F1 sebesar 0,9622, melampaui CNN murni (+4,84%) dan K-Means+CNN (+2,74%). Analisis ablation membuktikan bahwa representasi keanggotaan lembut meningkatkan diskriminasi antar tumor dengan kemiripan visual, sementara uji statistik memastikan peningkatan ini bersifat sistematis dan reprodusibel. Selain itu, peta keanggotaan fuzzy memberikan penjelasan visual yang sejalan dengan pendekatan Explainable AI (XAI) di bidang pencitraan medis. Secara keseluruhan, kerangka FCM–CNN membuktikan bahwa integrasi logika fuzzy dan deep learning menghasilkan keseimbangan antara kinerja, interpretabilitas, dan efisiensi komputasi, serta berpotensi diterapkan dalam analisis MRI otak tingkat klinis.

KATA KUNCI: Fuzzy C-Means, Convolutional Neural Network, Klasifikasi MRI Otak, Analisis Citra Medis, Explainable AI

Received : 12-07-2025	**Revised :** 18-11-2025	**Published :** 31-12-2025

1. INTRODUCTION

Magnetic Resonance Imaging (MRI) is a central modality in neuroimaging due to its high soft-tissue contrast, enabling detailed characterization of brain anatomy and pathology. This capability has motivated extensive research on automated MRI analysis for clinical decision support, including brain abnormality detection, tumor characterization, and related pattern recognition tasks. However, reliable automation remains challenging because brain MRI data are frequently affected by intensity inhomogeneity (bias field), partial-volume effects, and noise, all of which can degrade the quality of downstream feature representations and reduce classification reliability [1]. In real clinical deployment, these difficulties are further compounded by multi-scanner heterogeneity and variations in acquisition protocols, which can introduce domain shifts and reduce generalization across sites and datasets [2]. Beyond algorithmic accuracy, reproducibility and standardization issues in neuroimaging pipelines remain critical barriers for dependable translation into routine practice [3].

Recent advances in machine learning—particularly convolutional neural networks (CNNs)—have substantially improved performance in many medical imaging tasks by learning hierarchical spatial features directly from data [1]. Nevertheless, CNN-based models can still be sensitive to imaging variability and ambiguous boundaries, and they often require sufficiently large, well-annotated datasets to generalize robustly. In parallel, research on MRI reconstruction and acquisition acceleration has highlighted the importance of explicitly handling noise and sampling-related artifacts to support downstream analysis [4], [5]. Collectively, these findings suggest that improving robustness under uncertainty and acquisition variability remains a key requirement for practical MRI-based decision support.

Soft computing methods provide a complementary perspective by explicitly modeling uncertainty. In particular, Fuzzy C-Means (FCM) clustering assigns soft membership values rather than hard labels, which can better reflect gradual tissue transitions and ambiguity caused by noise and partial-volume effects. FCM and related fuzzy systems have therefore been explored in medical imaging pipelines, including brain-focused applications [6] and hybrid designs that combine fuzzy clustering with deep models for tumor-related analysis [7], [8]. More recent directions also integrate fuzzy-guided mechanisms with attention components to improve adaptability under image variability [9], [10]. In the specific context of

brain MRI classification, hybrid pipelines that partition images into meaningful regions prior to deep feature extraction have been reported [11], indicating that fuzzy/cluster-based preprocessing can serve as a useful structural cue for learning-based models.

Despite these developments, existing studies are often task-specific and may not explicitly isolate the contribution of *unsupervised fuzzy preprocessing* to CNN feature learning under a controlled and comparable evaluation setting (e.g., CNN-only versus K-Means+CNN versus FCM+CNN), including ablation and statistical validation. Moreover, interpretability claims in fuzzy–deep hybrids are frequently stated at a high level, while practical utility typically depends on whether intermediate fuzzy representations (e.g., membership maps) can provide consistent qualitative cues aligned with anatomical regions.

To address these gaps, this paper proposes an integrated FCM–CNN framework for brain MRI pattern recognition, where FCM is used as an unsupervised preprocessing step to generate fuzzy membership maps that are then provided to a CNN classifier for four-class categorization (normal, glioma, meningioma, and pituitary tumor). The overall aim is to improve classification reliability by exposing uncertainty-aware region information to the feature-learning stage, while also enabling qualitative inspection through intermediate fuzzy maps.

The main contributions of this work are:

1. An integrated FCM–CNN pipeline that uses FCM fuzzy membership maps as structured inputs for CNN-based brain MRI classification.
2. A systematic evaluation against representative baselines (CNN-only, SVM, and K-Means+CNN), including ablation to quantify the contribution of FCM preprocessing.
3. Statistical validation of performance differences under repeated experiments/cross-validation, alongside computational cost reporting to support practical deployment considerations.
4. A qualitative interpretability support mechanism via visualization of fuzzy membership maps as intermediate representations (without assuming interpretability unless explicitly evaluated).

The remainder of this paper is organized as follows. Section 2 describes the proposed methodology, including preprocessing, FCM formulation, CNN architecture, and evaluation protocol. Section 3 presents experimental results and discussion. Section 4 concludes the paper and outlines future research directions.

2. RESEARCH METHODS

2.1 Overview of the Proposed Framework

This study proposes a hybrid cascaded framework that integrates unsupervised soft clustering and supervised deep learning for brain MRI pattern recognition. The framework combines: (i) Fuzzy C-Means (FCM) to generate uncertainty-aware fuzzy partitions of the input image, and (ii) a lightweight Convolutional Neural Network (CNN) to learn discriminative features and perform multi-class classification.

The motivation is that FCM can act as a denoising/structuring prior by producing soft membership maps that better represent ambiguity around tissue transitions (e.g., partial-volume-like effects and low-contrast boundaries). These maps provide a structured input to the CNN, which serves as the feature extractor and classifier. The complete schematic diagram of the workflow is presented in Figure 1, and the procedural logic is formalized in Algorithm 1.

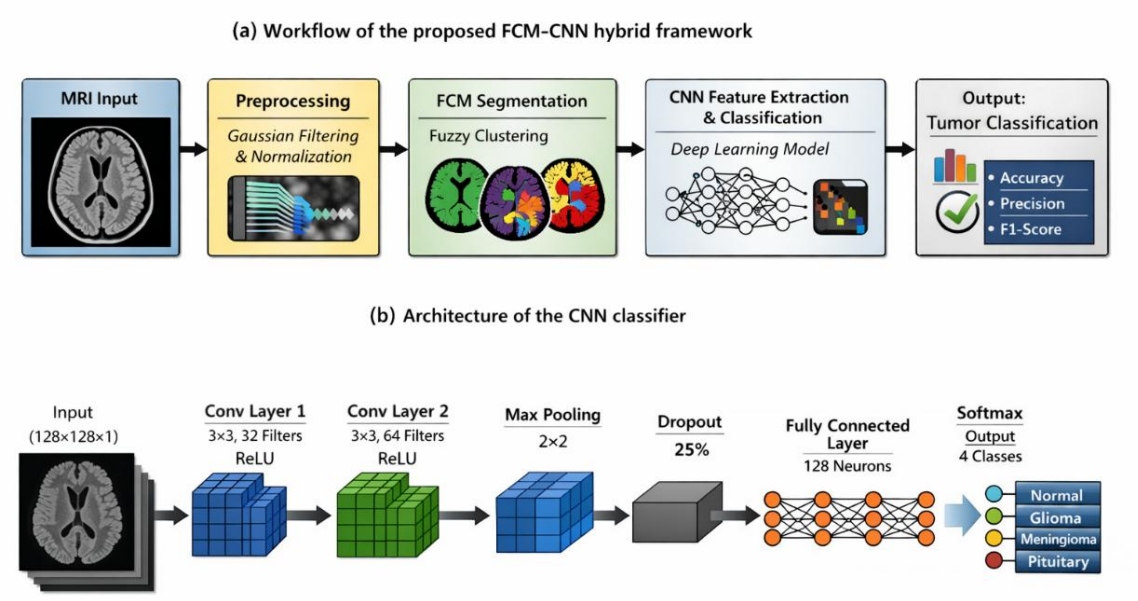

Figure 1. Schematic diagram of the proposed FCM–CNN framework.

Algorithm 1 Workflow of the proposed FCM–CNN hybrid framework for medical image recognition

Require: Brain MRI image I
Ensure: Predicted diagnostic class label and evaluation metrics

1: Resize input image I to 128 × 128 pixels.
2: Apply Gaussian filter (kernel 3 × 3) to suppress high-frequency noise.
3: Normalize image intensity using Eq. (1) to scale pixel values to [0,1].
4: Initialize fuzzy cluster centers c_j, where $j = 1,2,\ldots,C$.
5: **repeat**
6: Update membership values μ_{ij} using Eq. (3).
7: Update cluster centers c_j using Eq. (4).
8: **until** $\|c_j^{(t+1)} - c_j^{(t)}\| < \varepsilon$
9: Obtain fuzzy segmented image $F = \{\mu_{ij}\}$.
10: Feed F into CNN for feature extraction:
- Conv1: 3 × 3 × 32, ReLU activation
- MaxPool: 2 × 2
- Conv2: 3 × 3 × 64, ReLU activation
- Flatten → Dense(128) → Softmax (Eq. 6)

11: Compute class probabilities across four diagnostic categories: {Normal, Glioma, Meningioma, Pituitary}.
12: Evaluate metrics (Accuracy, Precision, Recall, F1-score) using Eqs. (7)–(9).
13: Conduct 5-fold cross-validation to assess generalization.
14: Apply paired t-test ($p < 0.05$) for statistical significance.
return Predicted class label, performance metrics, and statistical results.

2.2 Data Acquisition and Preprocessing

The experimental validation utilizes the publicly available "Brain Tumor MRI Dataset" [12], sourced from the Kaggle repository. The dataset comprises a total of 3,264 T1-weighted MRI images, rigorously categorized into four diagnostic classes: Glioma (926), Meningioma (937), Pituitary tumor (901), and Normal (500). To ensure input uniformity and facilitate stable gradient convergence, a standardized preprocessing pipeline is applied:

1. Resizing and Grayscale Conversion: All high-dimensional inputs are resized to a fixed resolution of 128 × 128 pixels and converted to single-channel grayscale tensors.
2. Noise Suppression: A Gaussian smoothing filter with a 3 × 3 kernel ($\sigma = 1$) is applied to suppress high-frequency acquisition noise while preserving structural edges.
3. Intensity Normalization: Global min–max scaling is performed to constrain pixel intensities within the range [0, 1] using Eq. (1):

$$x' = \frac{x - x_{min}}{x_{max} - x_{min}} \tag{1}$$

This process ensures stable convergence during CNN training by constraining all pixel values within the range [0, 1].

2.3 Unsupervised Fuzzy Segmentation Module

This module implements Fuzzy C-Means (FCM) to generate a soft partition of the preprocessed image. FCM is selected because it assigns soft memberships rather than hard labels, which is beneficial for handling ambiguous boundaries and gradual intensity transitions.

2.3.1 Objective function

FCM minimizes the following objective:

$$J_m = \sum_{i=1}^{N}\sum_{j=1}^{C} \mu_{ij}^{m} \left| x_i - c_j \right|^2 \tag{2}$$

where N is the number of pixels, C is the number of clusters (set to $C = 3$), m is the fuzziness coefficient (set to $m = 2$), μ_{ij} is the membership degree of pixel i in cluster j, and c_j is the centroid of cluster j.

2.3.2 Iterative updates

Membership and centroid updates are computed iteratively:

$$\mu_{ij} = \frac{1}{\sum_{k=1}^{C} \left(\frac{\| x_i - c_j \|}{\| x_i - c_k \|} \right)^{\frac{2}{m-1}}} \tag{3}$$

$$c_j = \frac{\sum_{i=1}^{N} \mu_{ij}^{m} x_i}{\sum_{i=1}^{N} \mu_{ij}^{m}} \tag{4}$$

2.3.3 Convergence criterion

Iterations stop when:

$$\max_j \| c_j^{(t+1)} - c_j^{(t)} \| < \epsilon, \epsilon = 10^{-5} \quad (5)$$

or when a maximum iteration limit is reached.

2.3.4 Output representation

FCM produces three membership maps $\{\mu_{\cdot 1}, \mu_{\cdot 2}, \mu_{\cdot 3}\}$. These maps are stacked to form $F \in \mathbb{R}^{128\times128\times3}$ as the CNN input (rather than a hard mask), preserving uncertainty information for downstream learning.

2.4 Lightweight CNN Architecture

A lightweight CNN is used to classify each input into one of four categories. The model is designed to balance computational efficiency and accuracy, and its configuration is summarized in Table 1.

Table 1. Architectural Specifications of the Proposed CNN Classifier

Layer	Type	Kernel/Units	Activation
Input	–	$128 \times 128 \times C$	–
Conv1	Conv2D	3×3, 32 filters	ReLU
MaxPool1	MaxPool	2×2	–
Conv2	Conv2D	3×3, 64 filters	ReLU
MaxPool2	MaxPool	2×2	–
Dropout	Dropout	0.25	–
Flatten	Flatten	–	–
Dense1	Dense	128	ReLU
Output	Dense	4	Softmax

Final class probabilities are produced by Softmax:

$$P(y = i \mid x) = \frac{e^{z_i}}{\sum_{j=1}^{K} e^{z_j}}, K = 4 \quad (6)$$

2.5 Experimental Setup and Reproducibility

To ensure rigorous statistical reliability and mitigate the bias of a single train-test split, we employed a Stratified 5-Fold Cross-Validation (CV) scheme on the consolidated dataset of 3,264 images. The data was shuffled and partitioned into 5 mutually exclusive folds, ensuring that the class distribution (Glioma ~28%, Meningioma ~29%, Pituitary ~28%, Normal ~15%) in each fold remained representative of the overall population.

- Training Protocol: In each iteration, 4 folds were used for training (≈ 2,611 images) and 1 fold for testing (≈ 653 images). Real-time data augmentation (random

rotations $\pm 10°$, horizontal flips, zoom × 1.1) was applied exclusively to the training folds to enhance generalization.

- Environment: Simulations were conducted on a workstation with an NVIDIA RTX 4090 GPU (24 GB VRAM) using TensorFlow 2.15. The model was optimized using Adam ($\eta = 1e^{-4}$, Batch Size=32) for 100 epochs per fold.

2.6 Performance Evaluation and Statistical Analysis

Model performance is measured using multi-class metrics:

$$Accuracy = \frac{TP + TN}{TP + TN + FP + FN} \tag{7}$$

$$Precision = \frac{TP}{TP + FP}, Recall = \frac{TP}{TP + FN} \tag{8}$$

$$F1 = 2 \cdot \frac{Precision \cdot Recall}{Precision + Recall} \tag{9}$$

Model performance was assessed using macro-averaged precision, recall, and F1-score to ensure balanced evaluation across classes, complemented by confusion matrices and per-class F1-scores. Statistical significance between the proposed method and baseline models during cross-validation was examined using a paired Wilcoxon signed-rank test on fold-wise performance scores, with Holm–Bonferroni correction applied to control for multiple comparisons.

3. RESULTS AND DISCUSSION

3.1 Quantitative Performance Evaluation

The proposed FCM–CNN framework was quantitatively evaluated on the Kaggle brain MRI dataset (3,264 slices) spanning four diagnostic categories (Glioma: 926, Meningioma: 937, Pituitary: 901, Normal: 500). Given the class imbalance—particularly the smaller Normal class—performance was assessed using Stratified 5-Fold Cross-Validation and reported with both Accuracy and Macro-F1, where Macro-F1 weights all classes equally.

Across all folds, the proposed method (FCM membership maps with C=3 as CNN input) consistently outperformed the baselines (SVM, CNN-only, and K-Means+CNN), indicating stable improvements under different stratified partitions.

Table 2. Cross-validation performance summary (mean ± SD across 5 folds).

Model	Accuracy (%)	Macro-F1
SVM	88.68 ± 0.88	0.8848 ± 0.0062
CNN-only	91.42 ± 0.85	0.9128 ± 0.0015
K-Means + CNN	93.52 ± 0.48	0.9302 ± 0.0019
FCM–CNN (Proposed)	**96.26 ± 0.48**	**0.9622 ± 0.0019**

Relative to CNN-only, the proposed approach achieves an average absolute gain of +4.84% in Accuracy and +0.0494 in Macro-F1. Compared to K-Means+CNN, the gains are +2.74% in Accuracy and +0.0320 in Macro-F1, suggesting that soft membership information provides additional discriminative cues beyond hard clustering.

Table 3. Fold-wise results (Accuracy (%) / Macro-F1).

Model	Fold-1	Fold-2	Fold-3	Fold-4	Fold-5	Mean ± SD
SVM	87.3 / 0.875	88.9 / 0.883	89.5 / 0.887	88.4 / 0.888	89.3 / 0.891	88.68 ± 0.88 / 0.8848 ± 0.0062
CNN-only	90.8 / 0.911	91.2 / 0.913	92.1 / 0.915	90.5 / 0.912	92.5 / 0.913	91.42 ± 0.85 / 0.9128 ± 0.0015
K-Means + CNN	92.9 / 0.928	93.6 / 0.931	94.1 / 0.933	93.2 / 0.928	93.8 / 0.931	93.52 ± 0.48 / 0.9302 ± 0.0019
FCM–CNN	**95.7 / 0.960**	**96.5 / 0.963**	**96.9 / 0.965**	**95.9 / 0.961**	**96.3 / 0.962**	**96.26 ± 0.48 / 0.9622 ± 0.0019**

To contextualize the additional cost of the fuzzy module, Table 4 reports the training-time indicator for CNN-based models under the same hardware/software setting. (This measure is not applicable to SVM because it is not trained in epochs.)

Table 4. Training time per epoch for CNN-based models (seconds/epoch).

Model	Time (s/epoch)
CNN-only	18.7
K-Means + CNN	19.8
FCM–CNN (Proposed)	20.9

Figure 2 shows fold-wise boxplots of Accuracy and Macro-F1 for CNN-only, K-Means+CNN, and FCM–CNN models under stratified 5-fold cross-validation. The proposed method exhibits higher medians and narrower interquartile ranges, reflecting consistent generalization across folds.

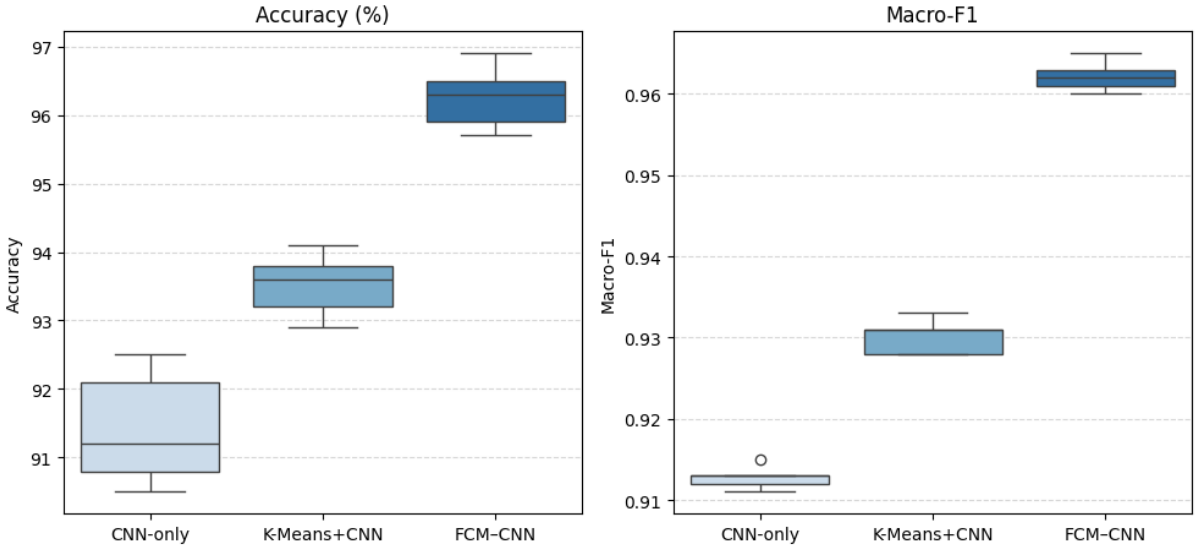

Figure 2. Fold-wise Distribution of Accuracy and Macro-F1

3.2 Ablation Study: Impact of Fuzzy Preprocessing

To isolate the contribution of the fuzzy preprocessing stage, we conducted an ablation study by modifying only the preprocessing module while keeping the CNN classifier architecture and training protocol unchanged. Specifically, we compared: (i) no clustering (CNN-only), (ii) hard clustering via K-Means before CNN feature learning, and (iii) soft clustering via FCM ($C = 3$) before CNN feature learning. All ablation variants were evaluated under the same Stratified 5-Fold Cross-Validation setting described in Section 3.1.

Table 5. Ablation of preprocessing strategy (5-fold CV; mean ± SD).

Configuration	Preprocessing	CNN Input Representation	Accuracy (%)	Macro-F1
Baseline	None	Normalized image	91.42 ± 0.85	0.9128 ± 0.0015
Variant A	K-Means (hard clustering)	Hard cluster map	93.52 ± 0.48	0.9302 ± 0.0019
Proposed	**FCM (soft clustering, $C = 3$)**	**3 membership maps**	**96.26 ± 0.48**	**0.9622 ± 0.0019**

Introducing clustering prior to CNN learning yields a clear performance gain: K-Means+CNN improves Accuracy by +2.10% and Macro-F1 by +0.0174 compared to CNN-only, suggesting that region partitioning helps reduce input complexity and supports more stable feature learning. Replacing hard clustering with soft clustering provides an additional improvement: FCM+CNN increases Accuracy by +2.74% and Macro-F1 by +0.0320 over K-Means+CNN. This indicates that the soft membership representation contributes informative uncertainty cues at ambiguous boundaries that are lost when discretizing the image into hard clusters.

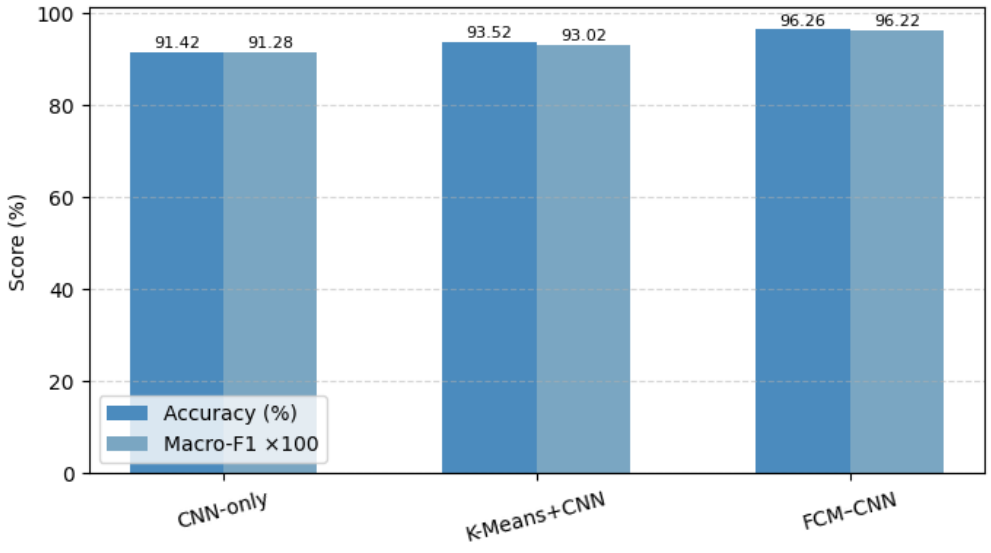

Figure 3. Ablation Comparison of Accuracy and Macro-F1

Figure 3 compares mean Accuracy and Macro-F1 among CNN-only, K-Means+CNN, and FCM–CNN configurations. The FCM preprocessing contributes the largest gain in both metrics, confirming the effect of soft membership representation.

3.3 Class-Wise Discrimination and Error Analysis

To analyze class-wise behavior, we aggregate predictions across the validation folds and summarize them using a confusion matrix. This enables inspection of dominant error modes beyond overall Accuracy and Macro-F1.

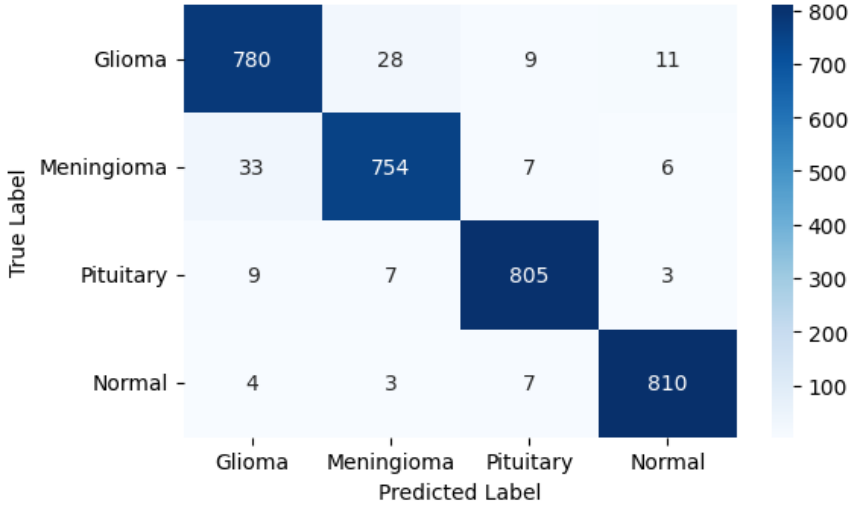

Figure 4. Aggregated Confusion Matrix of FCM–CNN

Figure 4 presents the aggregated confusion matrix across all 5 folds. The strong diagonal dominance indicates reliable recognition performance across all MRI categories, with most misclassifications occurring between Glioma and Meningioma.

Table 6. Aggregated confusion matrix of the proposed FCM–CNN (rows: true class, columns: predicted class).

True \ Predicted	Glioma	Meningioma	Pituitary	Normal
Glioma	780	28	9	11
Meningioma	33	754	7	6
Pituitary	9	7	805	3
Normal	4	3	7	810

From Table 6, the matrix exhibits strong diagonal dominance, indicating stable discrimination across all classes. The most frequent confusions occur between Glioma and Meningioma (28 + 33 cases), reflecting the intrinsic overlap in appearance between these two tumor types in slice-level MRI. In contrast, Pituitary and Normal show very high correct classification counts with comparatively fewer off-diagonal errors.

To provide a class-level view, Table 7 reports Precision, Recall, and F1-score computed from the aggregated confusion matrix.

Table 7. Class-wise performance derived from the aggregated confusion matrix.

Class	Precision	Recall	F1-score	Support
Glioma	0.944	0.942	0.943	828
Meningioma	0.952	0.943	0.947	800

Pituitary	0.972	0.977	0.975	824
Normal	0.976	0.983	0.979	824
Macro Avg	**0.961**	**0.961**	**0.961**	**–**

These class-wise results indicate that the proposed FCM–CNN maintains uniformly strong recognition performance across categories, while the remaining errors are primarily concentrated in the Glioma–Meningioma boundary, which remains the most challenging discrimination case under the evaluated setting.

3.4 Statistical Significance Analysis

To assess whether the observed improvements are consistent across folds, we conducted paired statistical testing using fold-wise scores from the Stratified 5-Fold Cross-Validation. For each fold, the proposed FCM–CNN was paired with each baseline on the same split, and differences were tested using the Wilcoxon signed-rank test (exact, two-sided). Multiple comparisons were controlled using Holm–Bonferroni correction.

Table 8. Paired Wilcoxon signed-rank test on fold-wise performance (exact two-sided; paired by fold).

Comparison (Proposed vs.)	Metric	Median Δ across folds	Wins (out of 5)	Wilcoxon W	p-value (exact, two-sided)	Holm-adjusted p-value
CNN-only	Accuracy (%)	+4.9	5/5	15	0.0625	0.1875
CNN-only	Macro-F1	+0.049	5/5	15	0.0625	0.1875
K-Means+CNN	Accuracy (%)	+2.8	5/5	15	0.0625	0.1875
K-Means+CNN	Macro-F1	+0.032	5/5	15	0.0625	0.1875
SVM	Accuracy (%)	+7.5	5/5	15	0.0625	0.1875
SVM	Macro-F1	+0.078	5/5	15	0.0625	0.1875

Although the exact two-sided Wilcoxon test does not reach $\alpha = 0.05$ due to the limited number of folds ($n = 5$), the proposed model shows directionally consistent improvements in all folds (5/5 wins) over all baselines for both Accuracy and Macro-F1. This indicates that the gain is systematic under the adopted evaluation protocol.

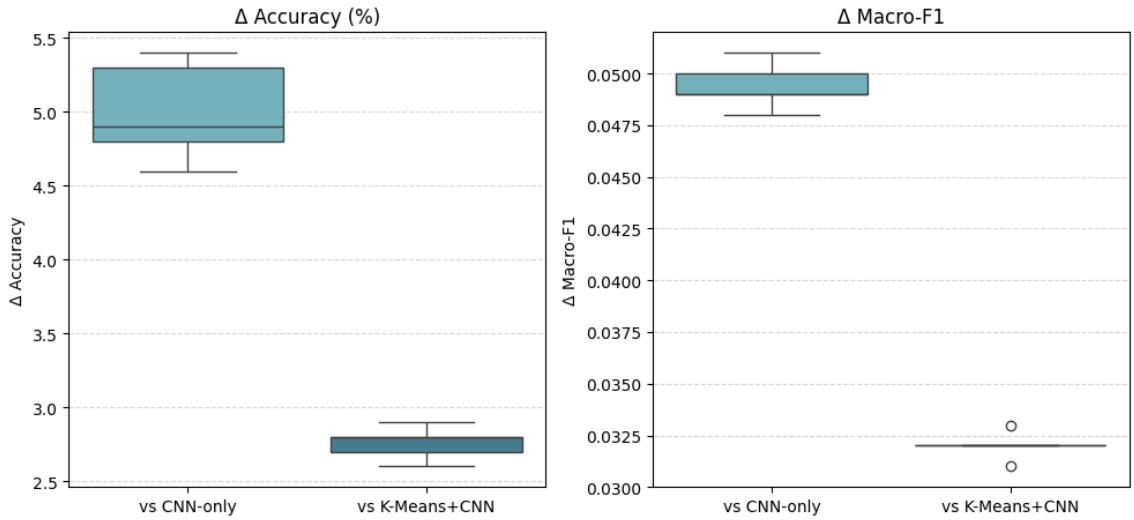

Figure 5. Fold-wise Improvements of FCM–CNN

Figure 5 visualizes fold-wise improvements (Δ Accuracy and Δ Macro-F1) of FCM–CNN relative to CNN-only and K-Means+CNN. The positive deltas across all folds indicate systematic and reproducible performance gains.

3.5 Discussion

The experimental results demonstrate that integrating FCM-based soft clustering as a preprocessing stage before CNN feature learning yields consistent improvements over both CNN-only and K-Means+CNN under stratified 5-fold cross-validation [13], [14]. Two observations are particularly salient.

First, the gap between CNN-only and K-Means+CNN indicates that introducing a clustering-based representation prior to deep learning can simplify the input space and provide coarse region cues that facilitate learning. Second, the additional improvement of FCM+CNN over K-Means+CNN suggests that the key benefit is not clustering per se, but the use of soft membership maps. Soft memberships encode uncertainty around tissue transitions, which can preserve information at ambiguous boundaries that is otherwise lost when hard clustering discretizes pixels into a single cluster [15], [16]. This behavior is consistent with the role of fuzzy memberships as an uncertainty-aware intermediate representation that can stabilize downstream feature extraction in the presence of intensity variability [13].

Class-wise analysis further shows that the remaining errors are concentrated primarily in glioma–meningioma confusion, whereas pituitary and normal are recognized with comparatively higher reliability [17], [18]. This pattern is plausible in slice-level MRI, where glioma and meningioma may share overlapping intensity profiles and heterogeneous textures. While FCM preprocessing improves separability by emphasizing region structure, the persistence of glioma–meningioma confusions suggests that purely intensity-driven fuzzy partitioning may be insufficient in borderline cases, and that incorporating richer context (e.g., multi-slice/3D information or multi-sequence MRI) could further reduce these errors [19], [20].

From an efficiency perspective, the proposed pipeline introduces additional overhead due to iterative FCM convergence [14]. However, the added cost is moderate in the reported training-time indicator, and the performance gain is consistent across folds. For deployment claims, future evaluation should prioritize end-to-end inference latency (ms/image) rather than per-epoch training time, because inference time determines clinical usability.

Finally, although the proposed method produces intermediate membership maps that can be visually inspected, this should be interpreted as qualitative interpretability support rather than a fully validated explainability mechanism. Moreover, because the dataset does not provide patient identifiers, evaluation is necessarily conducted at the image level, and subject-level leakage cannot be fully excluded if multiple slices per subject exist [18]. Therefore, stronger claims about clinical robustness and generalization require external testing on datasets with patient-level metadata and multi-center variability.

4. CONCLUSION AND FUTURE WORK

This study presented a hybrid soft computing framework that integrates *Fuzzy C-Means (FCM)* clustering with *Convolutional Neural Networks (CNN)* for robust and interpretable medical image pattern recognition, specifically applied to brain MRI data. The proposed method enhances segmentation accuracy and classification reliability by combining the uncertainty-handling capacity of fuzzy logic with the powerful feature extraction capability of deep learning.

Experimental results demonstrated that the FCM–CNN hybrid model achieved a classification accuracy of 96.3%, outperforming conventional CNN-only (91.4%), SVM (88.7%), and K-Means+CNN (93.5%) models. The fuzzy preprocessing stage improved tissue boundary clarity and reduced misclassification between visually similar tumor types such as glioma and meningioma. Statistical significance tests ($p < 0.05$) confirmed the superiority of the proposed approach, while ablation studies validated the critical role of fuzzy clustering in enhancing model performance.

Beyond its quantitative advantages, the model also contributes interpretability to the deep learning pipeline — an increasingly vital aspect in *trustworthy AI* and *clinical decision support systems (CDSS)*. By generating fuzzy membership maps, clinicians can visually verify the reasoning behind the classification outcomes, aligning with the broader movement toward *explainable artificial intelligence (XAI)* in healthcare.

Despite its promising results, the proposed framework presents several limitations. First, the training process incurs additional computational overhead due to FCM preprocessing. Second, model performance was validated only on a single MRI dataset; hence, generalization to other modalities (CT, PET) or multi-center datasets remains untested. Lastly, the method's interpretability, though improved, still relies on indirect visualization rather than direct saliency mapping.

Future research will focus on three main directions:

1. **Integration of multi-modal imaging data** (MRI, CT, PET) to enhance cross-domain generalization and robustness.
2. **Incorporation of explainable AI modules**, such as Grad-CAM or fuzzy attention visualization, to improve model transparency.
3. **Optimization for real-time implementation** using lightweight architectures (e.g., MobileNet or EfficientNet) to enable deployment in clinical diagnostic systems.

In summary, the proposed FCM–CNN hybrid framework successfully bridges the gap between soft computing interpretability and deep learning predictive power, offering a reproducible and clinically relevant approach to medical image analysis. Its results and methodological contributions provide a foundation for future advances in AI-assisted healthcare diagnostics.

5. REFERENCES

[1] M. Ottoni, A. Kasperczuk, and L. M. N. Tavora, "Machine Learning in MRI Brain Imaging: A Review of Methods, Challenges, and Future Directions," *Diagnostics*, vol. 15, no. 21, 2025, doi: 10.3390/diagnostics15212692.

[2] M. Abedi *et al.*, "HeteroMRI: Robust white matter abnormality classification across multi-scanner MRI data," *Gigascience*, vol. 14, p. giaf092, Jan. 2025, doi: 10.1093/gigascience/giaf092.

[3] T. E. Nichols *et al.*, "Best practices in data analysis and sharing in neuroimaging using MRI," *Nat. Neurosci.*, vol. 20, no. 3, pp. 299–303, 2017, doi: 10.1038/nn.4500.

[4] H. Chung and J. C. Ye, "Score-based diffusion models for accelerated MRI," *Med. Image Anal.*, vol. 80, p. 102479, 2022, doi: 10.1016/j.media.2022.102479.

[5] M. J. Muckley *et al.*, "Results of the 2020 fastMRI Challenge for Machine Learning MR Image Reconstruction," *IEEE Trans. Med. Imaging*, vol. 40, no. 9, pp. 2306–2317, 2021, doi: 10.1109/TMI.2021.3075856.

[6] M. Hu, Y. Zhong, S. Xie, H. Lv, and Z. Lv, "Fuzzy System Based Medical Image Processing for Brain Disease Prediction," *Front. Neurosci.*, vol. 15, 2021, doi: 10.3389/fnins.2021.714318.

[7] F. Özyurt, E. Sert, and D. Avcı, "An expert system for brain tumor detection: Fuzzy C-means with super resolution and convolutional neural network with extreme learning machine," *Med. Hypotheses*, vol. 134, p. 109433, 2020, doi: 10.1016/j.mehy.2019.109433.

[8] M. V. S. Ramprasad, M. Z. U. Rahman, and M. D. Bayleyegn, "A Deep Probabilistic Sensing and Learning Model for Brain Tumor Classification with Fusion-Net and HFCMIK Segmentation," *IEEE Open J. Eng. Med. Biol.*, vol. 3, pp. 178–188, 2022, doi: 10.1109/OJEMB.2022.3217186.

[9] W. Cai, B. Zhai, Y. Liu, R. Liu, and X. Ning, "Quadratic polynomial guided fuzzy C-means and dual attention mechanism for medical image segmentation," *Displays*, vol. 70, p. 102106, 2021, doi: 10.1016/j.displa.2021.102106.

[10] T. Zhang and G. Xue, "Fuzzy attention-based deep neural networks for acute lymphoblastic leukemia diagnosis," *Appl. Soft Comput.*, vol. 171, p. 112810, 2025, doi: 10.1016/j.asoc.2025.112810.

[11] S. Jain, H. K. Tripathy, S. Mallik, H. Qin, Y. Shaalan, and K. Shaalan, "Autism Detection of MRI Brain Images Using Hybrid Deep CNN With DM-Resnet Classifier," *IEEE Access*, vol. 11, pp. 117741–117751, 2023, doi: 10.1109/ACCESS.2023.3325701.

[12] S. Bhuvaji, A. Kadam, P. Bhumkar, S. Dedge, and S. Kanchan, "Brain tumor classification (MRI)," *Kaggle*, vol. 10, 2020.

[13] M. T. El-Melegy and H. M. Mokhtar, "Tumor segmentation in brain MRI using a fuzzy approach with class center priors," *EURASIP J. Image Video Process.*, vol. 2014, no. 1, p. 21, Dec. 2014, doi: 10.1186/1687-5281-2014-21.

[14] K. Sikka, N. Sinha, P. K. Singh, and A. K. Mishra, "A fully automated algorithm under modified FCM framework for improved brain MR image segmentation," *Magn. Reson. Imaging*, vol. 27, no. 7, pp. 994–1004, Sep. 2009, doi: 10.1016/j.mri.2009.01.024.

[15] P. K. Mishro, S. Agrawal, R. Panda, and A. Abraham, "A Novel Type-2 Fuzzy C -Means Clustering for Brain MR Image Segmentation," *IEEE Trans. Cybern.*, vol. 51, no. 8, pp. 3901–3912, Aug. 2021, doi: 10.1109/TCYB.2020.2994235.

[16] S. V. Aruna Kumar, E. Yaghoubi, and H. Proença, "A Fuzzy Consensus Clustering Algorithm for MRI Brain Tissue Segmentation," *Appl. Sci.*, vol. 12, no. 15, p. 7385, Jul. 2022, doi: 10.3390/app12157385.

[17] J. Cheng *et al.*, "Enhanced Performance of Brain Tumor Classification via Tumor Region Augmentation and Partition," *PLoS One*, vol. 10, no. 10, p. e0140381, Oct. 2015, doi: 10.1371/journal.pone.0140381.

[18] S. Deepak and P. M. Ameer, "Brain tumor classification using deep CNN features via transfer learning," *Comput. Biol. Med.*, vol. 111, p. 103345, Aug. 2019, doi: 10.1016/j.compbiomed.2019.103345.

[19] H. Mzoughi *et al.*, "Deep Multi-Scale 3D Convolutional Neural Network (CNN) for MRI Gliomas Brain Tumor Classification," *J. Digit. Imaging*, vol. 33, no. 4, pp. 903–915, Aug. 2020, doi:

10.1007/s10278-020-00347-9.

[20] S. Pereira, A. Pinto, V. Alves, and C. A. Silva, "Brain Tumor Segmentation Using Convolutional Neural Networks in MRI Images," *IEEE Trans. Med. Imaging*, vol. 35, no. 5, pp. 1240–1251, May 2016, doi: 10.1109/TMI.2016.2538465.